N O T I C E

THIS DOCUMENT HAS BEEN REPRODUCED FROM
MICROFICHE. ALTHOUGH IT IS RECOGNIZED THAT
CERTAIN PORTIONS ARE ILLEGIBLE, IT IS BEING RELEASED
IN THE INTEREST OF MAKING AVAILABLE AS MUCH
INFORMATION AS POSSIBLE

PULL-OUT OF FIBERS FROM COMPOSITE MATERIALS
AT HIGH RATE OF LOADING

S. Amijima and T. Fujii

1. Report No. NASA TM-76530	2. Government Accession No.	3. Recipient's Catalog No.
4. Title and Subtitle PULL-OUT OF FIBERS FROM COMPOSITE MATERIALS AT HIGH RATE OF LOADING		5. Report Date MARCH 1981
		6. Performing Organization Code
7. Author(s) S. Amijima and T. Fujii		8. Performing Organization Report No.
		10. Work Unit No.
9. Performing Organization Name and Address SCITRAN Box 5456 Santa Barbara, CA 93108		11. Contract or Grant No. NASw 3198
		13. Type of Report and Period Covered Translation
12. Sponsoring Agency Name and Address National Aeronautics and Space Administration Washington, D.C. 20546		
		14. Sponsoring Agency Code

15. Supplementary Notes Translation of article from:
Journal of Japan Society of Materials Science, vol. 28, Nov. 1979, p 1091-97. (A80-19909)

16. Abstract

Numerical and experimental results are presented on the pullout phenomenon in composite materials at a high rate of loading. The finite element method was used, taking into account the existence of a virtual shear deformation layer as the interface between fiber and matrix. Experimental results agree well with those obtained by the finite element method. Numerical results show that the interlaminar shear stress is time-dependent, in addition, it is shown to depend on the applied load-time history. Under step pulse loading, the interlaminar shear stress fluctuates, finally decaying to its value under static loading.

17. Key Words (Selected by Author(s))	18. Distribution Statement Unclassified - Unlimited		
19. Security Classif. (of this report) Unclassified	20. Security Classif. (of this page) Unclassified	21. No. of Pages 18	22. Price

PULL-OUT OF FIBERS FROM COMPOSITE MATERIALS
AT HIGH RATE OF LOADING

S. Amijima[#] and T. Fujii[##]

1.   Introduction

The pull-out phenomenon of fibers from a matrix is an
important problem closely related to the stress transmission
mechanism and fiber stripping processes in composite materials.
This phenomenon is also a crucial factor of the impulsively
absorbed energy, for example, obtained from impulse-tests on
isots [1,2], as has been already pointed our by Outwater [3].
Lawrence investigated [4] the pull-out phenomenon of fibers from
matrix layers under static loading. However, for a high rate of
loading, it is often insufficient to rely only on the usual anal-
ysis of static loading. Namely, in static analysis shear stress
waves propagating within a material have not been considered.
Therefore, we investigated the pull-out phenomenon of fibers from
composite materials at high rates of loading, numerically and
experimentally, taking into account propagation of stress waves
within materials and existence of a virtual shear deformation
layer as an interface between a fiber and the matrix.

2.   A pull-out model and equations of motion

Let us consider a one-dimensional model of Figure 1a to
examine the pull-out phenomenon of fibers from fiber-enforced
composite materials (or piled boards). In the model, two differ-
ent layers are connected by a massless shear deformation layer
(an adhesive layer). Through this shear layer propagates the
shear stress that is proportional to relative displacement and
inversely proportional to the layer thickness. The shear layer
(the adhesive layer) in the model can be a matrix layer, or a
kind of shear stress propagation layer (transition layer) at
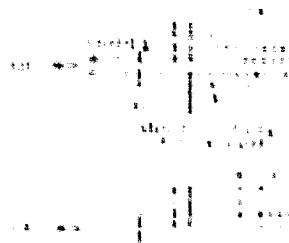the interface between fibers and the matrix, if one considers

---

Material 2 as a matrix. In the one-dimensional model, Figure 1a
and 1b are equivalent to each other.

Figure 1. Idealized
pull-out model

If a fiber is pulled out impulsively at one end, the load
propagates through the fiber as a stress wave and reaches a dis-
continuous junction. For static loading, one can analyze forces
acting on a fiber-matrix interface and stress variations within
the fiber only by examining balance of forces without consider-
ing the inertia of a material. However, for dynamical loading,
where stress waves propagate, one has to consider balance of
forces taking into account the inertia of the material, that is,
equations of motion. For simplicity, let us assume that layers
are flat and two-dimensionality can be ignored and consider pro-
pagation of stress waves in one dimension. From Figure 2 we see
that, as a pull-out stress wave reaches a discontinuous junction,
equations of motion are written as

$$\rho_1 A^{(1)} \frac{\partial^2 u^{(1)}}{\partial t^2} = \cdots = E_1 A^{(1)} \frac{\partial^2 u^{(1)}}{\partial x^2} \tag{1}$$

$$\rho_2 A^{(2)} \frac{\partial^2 u^{(2)}}{\partial t^2} = \cdots = E_2 A^{(2)} \frac{\partial^2 u^{(2)}}{\partial x^2} \tag{2}$$

Figure 2. Components
of forces
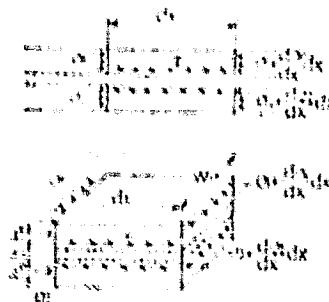
where u, E and ρ are the displacement, Young's modulo and the
density for each material, respectively, while the suffix 1 or
2 corresponds to the material 1 or 2. Also $A^{(1)}$ and $A^{(2)}$ are

cross sections of materials, given respectively by

$$A^{(1)} = \pi b^2, \quad A^{(2)} = \pi (c^2 - b^2)$$

G stands for the stiffness (shear elasticity) of a shear layer.

3. Numerical analysis

It is extremely difficult to solve Equations (1) and (2) analytically. They have been solved only under limited boundary conditions [5]. It seems almost impossible to obtain an analytical solution for the pull-out phenomenon, since the boundary condition at discontinuity is complex. Therefore, in order to obtain a realistic solution we analyzed equations numerically. Although any of the differential methods, the method of characteristic curves or the finite element method based on the Hamilton principle, may be applicable to this problem, we have employed the finite element method.

According to the Hamilton's principle, Equations (1) and (2) are equivalent to a functional Hamiltonian given by

$$H = \int \int \left[\frac{1}{2} \rho^{(1)} A^{(1)} \left(\frac{\partial u^{(1)}}{\partial t} \right)^2 + \frac{1}{2} \rho^{(2)} A^{(2)} \left(\frac{\partial u^{(2)}}{\partial t} \right)^2 \right. $$
$$- \frac{1}{2} E^{(1)} A^{(1)} \left(\frac{\partial u^{(1)}}{\partial x} \right)^2 + \frac{1}{2} E^{(2)} A^{(2)} \left(\frac{\partial u^{(2)}}{\partial x} \right)^2 $$
$$\left. - \frac{1}{2} \frac{G b^2}{h} (u^{(2)} - u^{(1)})^2 \right] dx \, dt \tag{3}$$

As shown in Figure 3, the triple layer junction of fiber-shear layer-matrix is meshed into finite number of elements. Let us denote two nodal points of the i-th element as i and i+1 and write its length as L. Displacements of the point i at time t for both materials 1 and 2 are written as

$$u_i^{(1)} = u^{(1)}(i, t), \quad u_i^{(2)} = u^{(2)}(i, t) \tag{4}$$

Figure 3. Finite
element mesh
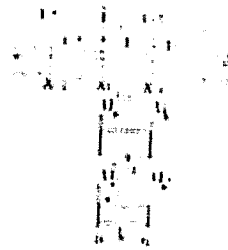
For displacements of the point i+1, one writes

$$u_{i+1}^{(i)} = u^{(i)}(x_i + l_i, t), \quad u_{i+1} = v^{(i)}(x_i, t) \tag{5}$$

Assuming linear variations of displacements within an element
and interpolating by a linear equation of the two nodal points'
displacements, one may obtain displacements within the i-th
element as

$$u^{(i)} = \frac{l_i - x}{l_i} u_i^{(i)} + \frac{x}{l_i} u^{(i)} \tag{6}$$

$$v^{(i)} = \frac{l_i - x}{l_i} u_i^{(i)} + \frac{x}{l_i} v^{(i)} \tag{7}$$

Substitute Equations (6) and (7) into Equation (3). Take var-
iations and set $\delta\pi = 0$. By adding an external force on the nodal
points, one gets the equation of motion for the element

$$[m]\frac{d^2}{dt^2}\{u\} + [k]\{u\} = \{f\} \tag{8}$$

where $\{u\}$ and $\{f\}$ are the nodal point displacement vector and
an external force vector at the point, respectively. Their com-
panies are given by

$$\{u\}^T = \{u_i^{(i)}, u_i^{(i)}, u_{i+1}^{(i)}, u_{i+1}^{(i)}\} \tag{9}$$

$$\{f\}^T = \{f_i^{(i)}, f_i^{(i)}, f_{i+1}^{(i)}, f_{i+1}^{(i)}\} \tag{10}$$

An element mass matrix [m] and the stiffness matrix [k] are
given respectively by

$$[m] = \frac{l}{6}\begin{bmatrix} 2A\rho^{(i)} & 0 & A\rho^{(i)} & 0 \\ 0 & 2A\rho^{(i)} & 0 & A\rho^{(i)} \\ A\rho^{(i)} & 0 & 2A\rho^{(i)} & 0 \\ 0 & A\rho^{(i)} & 0 & 2A\rho^{(i)} \end{bmatrix} \tag{11}$$

4

$$\text{(12)}$$

These are called a consistent mass matrix and a consistent stiffness matrix. Instead one may use lumped matrices for simplicity. They are given by

$$\text{(13)}$$

$$\text{(14)}$$

4. Experiments

We have experimented with the impulsive pull-out phenomenon using pull-out test specimens. Results will be later compared with those from numerical analysis by the finite element method.

4.1. Test specimens

Figure 4 shows the shape and the size of a test specimen as well as locations of strain gauges attached to it. A shear layer is formed by epoxy-adhesives. To investigate the effect due to the thickness of a shear layer, we used two kinds of test specimens, one with a 0.05 mm thick shear layer and another with 1 mm thickness. Both materials 1 and 2 are made of aluminum. We used commercially available epoxy-glues (Araldite) as adhesives.
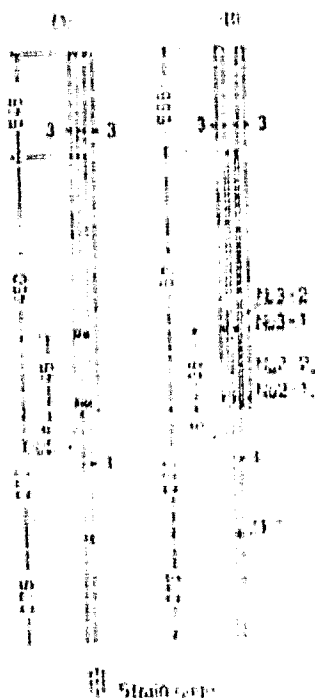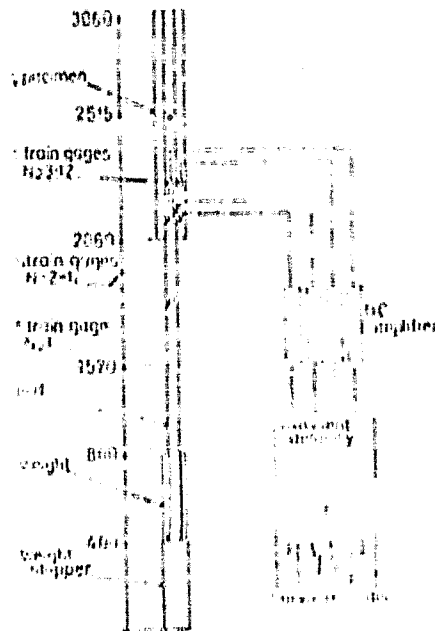
Figure 4.   Test specimens   Figure 5.   Experimental
apparatus

4.2.   Experimental apparatus

Figure 5 shows the apparatus of our experiments.   Let a
weight free-fall from the height of 700 mm and collide with a
stopper.   The collision generates stress in the rod until the
weight leaves the stopper.   The stress then propagates as a
stress wave towards a test specimen check.   When the stress wave
reaches the check, a part of it is transmitted into the Material
1, while the rest propagates back inside the rod as a reflected
stress wave.   The transmitted wave inside the Material 1 later
arrives at the adhesive junction with Material 2, and the phen-
omenon of an impulsive pull-out takes place.   Though the shear
stress at the interface between a fiber and the matrix is a
crucial factor in the phenomenon of pull-out of fibers in com-
pound materials, it is extremely difficult to measure this shear
stress or shear strain.   Instead, we have measured for simplicity

6

time variations of longitudinal strains for Materials 1 and 2
using accurate strain gauges and compared with numerical results.
Signals from strain gauges were amplified by a DC-amplifier
(Shinko DA-4007F; Frequency quality 50kHz/±3 db) and then
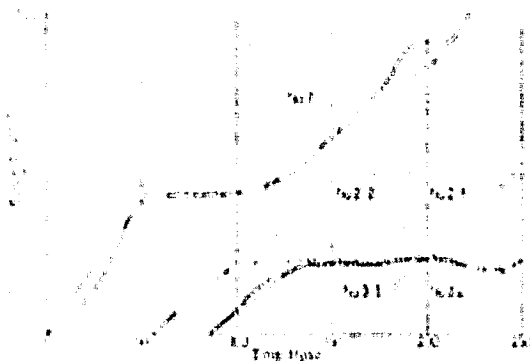recorded in digital memories. Strain gauges were 2 mm long
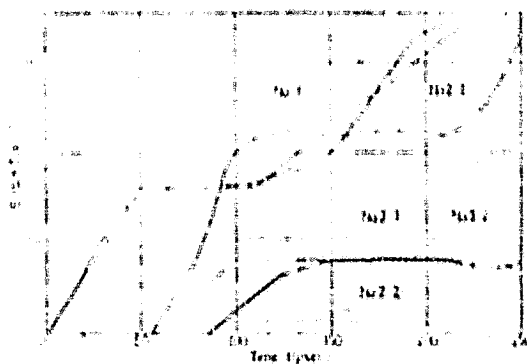(Kyowa KFC-2-11).

Figure 6. Stress wave records of A specimen

Figure 7. Stress wave records of B specimen

5. Results and discussions

5.1. Experimental results

Figures 6 and 7 show time variation of strains at each gauge location in test specimens A and B measured in the impulsive pull-out test. Here time is set at $t = 0$ when the front of a stress wave σ_1 in the Material 1 reaches the gauge number 1. σ_1 remains constant (with a constant stress magnitude) only during the first interval (or about 160 µsec) when the stress wave goes and returns between two ends of the stopper. Then the stress wave is transmitted and reflected multiply at both ends of the stopper and σ_1 starts to behave in a complex pattern. σ_1 is an almost step-like stress wave if the collision between a weight and a stopper is perfect, as both of them have homogeneous cross sections normal to the longitudinal direction. However, as is shown in Figures 6 and 7, σ_1 does not rise sharply as step-like, indicating an imperfect collision. The pulse is actually a ramp type with a pulse rise time of about 50 µsec. Furthermore, as is obvious in Figure 4, it is only until about 100 µsec counting from the wave front of σ_1 when only σ_1 is observed at the location of a gauge number 1. After this interval, σ_1 will be superimposed with its reflection at an predict the pattern of σ_1 any longer. Even if σ_1 is constant in time, the output from the No. 1 gauge will vary. Indeed as recorded in Fig. 6 and 7, the strain signal from the No. 1 gauge increased after 100 µsec. This increase must be due to the super-imposition of reflected waves from the adhesive junction. From the rate of increase, one may infer that σ_1 remains roughly constant until 160 sec. If the shear layer has zero thickness or its stiffness G is infinite, and the

8

compound material is assumed as a uniformly structured single
body, variations of stress waves may be treated by the theory of
elasticity stress wave propagation in one dimension [6]. For
our experimental specimen σ_T (transmitted stress wave) = ½ σ_1.
σ_R (reflected stress wave) = ½ σ_1. Dot-dash lines in Figures 6
and 7 are for predictions obtained from the one-dimensional wave
propagation theory, assuming a uniform structure for the adhesive
junction. In this computation, the incoming stress wave is taken
to be a ramp type pulse with a rise time of 50 μsec. By comparing
theoretical results in one dimensional wave theory with experi-
mental results, one finds that results from the specimen A with
a very thin adhesive layer agree well with theoretical predictions.

From comparison of two types of specimens A and B, one recog-
nizes the significant difference in values of no.2-2. While the
strain observed in an A specimen is consistent with that of one
dimensional theory, it hardly propagates in a B specimen that has
a thick shear layer. Apparently, the difference is attributed to
the thickness of shear layers. The magnitude of the shear stress
transmitted to the Material 2 from the Material 1 is inversely
proportional to the thickness b. For small b, the transmitted
shear stress is large, and two materials separated by an adhesive
layer form nearly uniform single body structure. Even though the
A specimen hints the similar tendency, we found that the strain
measured at No.2-1 in the material, particularly in the B speci-
men, is larger than not only the theoretical prediction, but the
incoming stress wave itself. If the shear layer is thinner and
the whole adhesive junction can be regarded as a single body, then
wave reflection takes place at the discontinuity where cross section
changes and the wave magnitude passing through no.2-1 have to be
smaller than the incoming wave. However, experimentally the
strain at No.2-1 is larger than the incoming wave. For the thick
shear layer the shear stress acting on the layer is small. It is
not transmitted to the material immediately, even after it

propagates through the Material 1 and reaches the adhesive junctions. While the incoming stress wave stays in the Material 1 inside of the junction, it transmits the stress to Material 2. When the force i. transmitted to Material 2 via shear stress, Material 1 also receives its reaction and the gauge no. 2-1 installed deeply in the junction records the strain (stress) larger than not only theoretical predicted σ_T transmitted wave, but the incoming stress wave σ_I itself. That is to say, the reflection plane for stress waves shifts effectively inward. If the shear layer gets thicker, the effective reflection plane moves further inward. Accordingly, an incoming wave penetrates into Material 1 inside of the junction and then is superimposed with its reflections. Then it is within an adhesive junction where the first large stress acts on Material 1. If Material 1 breaks down a little more than the incoming stress, then the shear breakdown of fibers could happen inside of this junction. At any rate, the one-dimensional theory may be sufficient to describe the stress far from the layer within the junction. But it fails to explain the details, much less the shear stress acting on a shear layer, that could be examined only by numerical analysis.

5.2 Numerical analysis results

As is clear from Figures 6 and 7, the stress caused by the impulse of a fallen weight in a pull-out material (fiber) may be approximated in terms of a ramp type pulse with a pulse rise time of 50 µsec. Therefore, we have examined in numerical analysis two types of loadings, one with a ramp type pulse of 50 µsec, and another with an extremely sharp step pulse. We used the following parameters:

Young's modulus (for Al) $E = 7000$ (kg/mm^2)
Density (for Al) $\tau = 2.75$ (g/cm^3)
Gravity acceleration $g = 9.8$ (m/s^2)
Shear elasticity (for Araldite) $G = 50$ (kg/mm^2)

We assumed a lumped mass matrix of Equation (13) and a consistent stiffness matrix, Equation (12). Runge-Kutta-Gill numerical method was employed to integrate equations of motion, Equation (8), while a unit interval for time integration is taken to be about 1/5 of the time required for the stress to pass through a finite element. Taking into consideration the phenomenon of wave propagation, we have divided the model in the figure into finite elements uniformly. We have used a computer HITAC 8300 (with memory capacity of 145 kb).

5.2.1 Ramp type pulse

In order to make a valid comparison with experiments, computation was done for the model in Figure 8a, which approximates the actual experimental specimen. Stress of a ramp type pulse with a rise time $T = 50$ μsec is assumed to act on the pull-out side of the model. The magnitude of the stress is taken to be 0.5 kg/mm^2. The length of an element is 2 mm for this computation. We analyzed the pull-out phenomenon as variations of strain at various sites in the model, until the reflected wave arrives there either from the loading end or from another freeend.
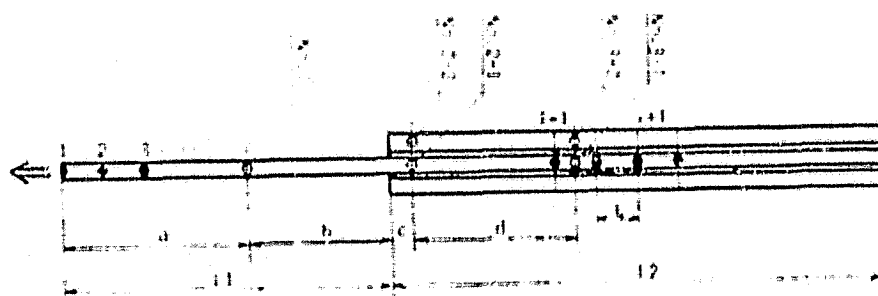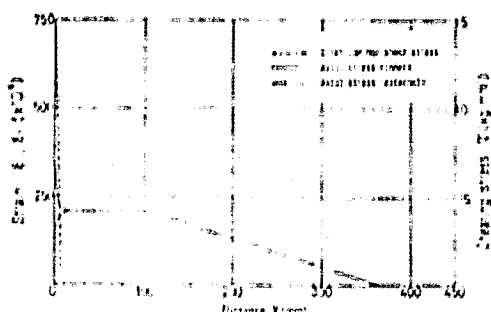

o   Calculated points

●   Nodal points

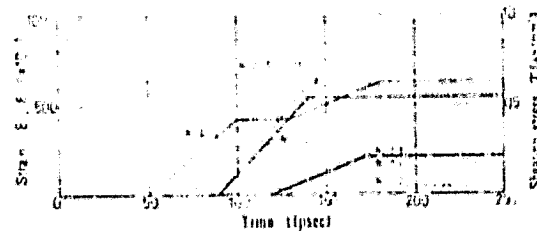|	1	11	12		L	l	l
A		450	450	250	250	1	150
B	1	160	250	80	80	0.5	150

Figure 8. Finite element model for calculation
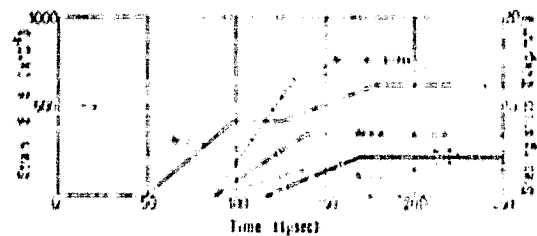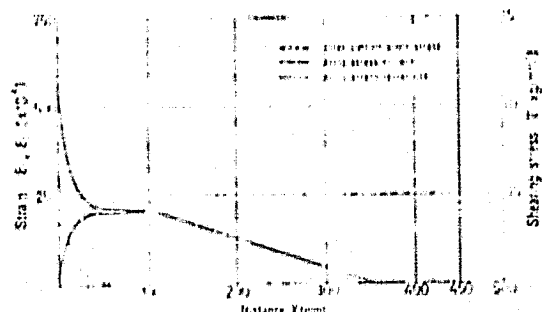
(a) Strain and shear stress time histories.

(b) Strain and shear stress distributions at $t = 100\mu sec$.

Figure 9. Calculated results of strains and shear stress in shear layer for A specimen: In case of ramp type pulse.

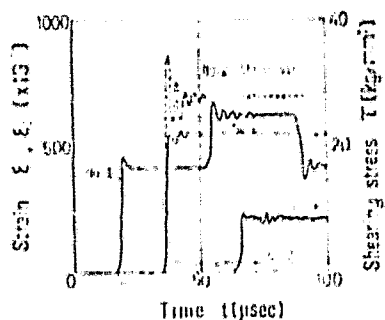(a) Strain and shear stress time histories.

(b) Strain and shear stress distributions at $t = 100\mu$.

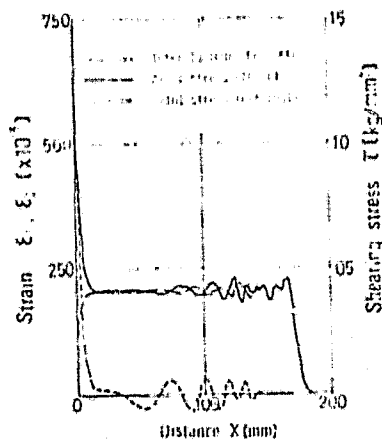Figure 10. Calculated results of strains and shear stress in shear layer for B specimen: In case of ramp type pulse.

Results are shown in Figures 9 and 10 for the shear layer thickness b = 0.05 mm and b = 1 mm, respectively. The time t is clocked from the instance the load is applied impulsively at the loading end. From the numerical curves agreement is remarkable qualitatively as well as quantitatively with experiments, except for the gauge No. 2-1 for the shear layer of b = 0.05mm. It could explain even smaller patterns at No.2-2, that is, the effect of a shear deformation layer which could not be understood in one-dimensional stress wave propagation theory with aforementioned single body hypothesis. The largest shear stress exists at the pull-out end, regardless of the shear layer thickness. For a pulse of a long rise time 50 μsec, the shear stress increases at the arrival of stress wave and when the stress remains constant it also stays constant equal to the one under static loading. Small fluctuations are observed only towards the end of a ramp pulse where the incoming stress wave vanishes discontinuously. These oscillations get slower for a thicker shear layer. Oscillations are more visible under a step pulse loading, as will be discussed below.
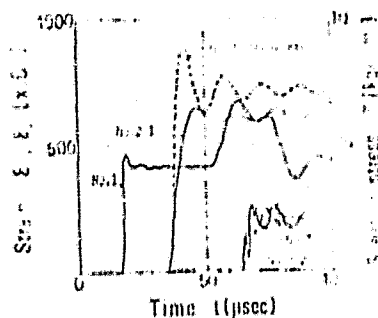
5.2.2 Step pulse

The most interesting phenomenon of the impulsive pull-out is found under a step pulse loading where an incoming stress is applied more abruptly than the ramp type pulse in order to approximate a literally impulsive loading. Numerical analysis was made for the case where an incoming step pulse is realized with an extremely quick rise time T = 1 μsec on one end of the pull-out material (fiber). The model used in the analysis is shown in Figure 8b. To obtain an approximate solution for wave quations Equations (1) and (2) for a sharply rising pulse, using the finite element method one has to solve an equivalent oscillatory equation, Equation (14), where all the masses of waves with infinite number of degrees of freedom are concentrated on every nodal point that counts finite. For a better approximation, for a sharper pulse one has to use as fine a division for
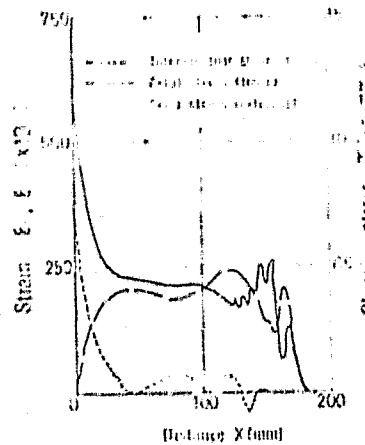
(a) Strain and shear stress time histories.

(b) Strain and shear stress distribution at t = 70 μsec.

(a) Strain and shear stress time histories.

(b) Strain and shear stress distributions at t = 70 μsec.

Figure 11. Calcualted results of strains and shear stress in shear layer for A specimen: in case of step pulse.

Figure 12. Calculated results of strains and shear stress in shear layer for B specimen: in case of step pulse.

14

each element as possible. We solved the set of differential
equations numerically using the Runge-Kutta-Gill method. From
consideration of the computer memory capacity and in order to
minimize the number of elements to avoid a large accumulation
of errors in the numerical method, we took the element length
of L = 1 mm. Thus, one can examine only a short time interval
in the pull-out phenomenon, yet this interval is long enough to
understand the transitional phenomenon. Figure 11 shows numer-
ical results for a b = 0.05 mm thick shear layer. One may notice
a few over chutes at the top of the strain wave at the no. 1 cite
sensitive to an incoming stress wave. These may be unavoidable
errors in the finite element method for wave equations. Although
they cannot be ignored for a detailed study, they are negligible
for an understanding of a global picture of the pull-out pheno-
menon. The inter-laminar shear stress fluctuates in time. The
fluctuation is much less visible in response to a ramp type pulse.
The fluctuation in inter-laminar shear stress finally decays to
the value under static loading. On the other hand, the impulsive /67
pull-out shear stress reaches a 20% larger value over the static
case in a transitional response period. Also, the stress varia-
tion along a fiber is more complex. One may assume that the fluc-
tuation of the shear stress is generated in the adhesive junction
in the following mechanism. Firstly, an injected stress wave
propagating in a fiber transmits the force towards the outer
material, and pulls it abruptly through the shear layer, but the
outer material cannot respond to it due to its inertia and then
the shear stress increases. Within a fiber, particles move along
the pulled direction first, but then they are decelerated. Nextly,
the outer material starts being pulled, the relative displacement
between the material and the fiber gets smaller and the shear
stress also decreases. Particles in the outer material, by iner-
tia, keep moving in the pulled direction, and the shear stress
reduces further. Then the decrease of the stress forces the par-
ticle deceleration that is caused by the strong shear stress
decrease. Consequently, the shear stress increases again in the
shear layer. This whole cycle repeats many times and there is a

fluctuation of the inter-laminar shear stress. Therefore, the fluctuation must depend on the thickness of a shear layer. As is seen in Figure 12, it is less frequent for a 1 mm thick shear layer. This frequency is quite insensitive to an element length as long as the variation of the division size for finite elements is sufficiently less frequent. This insensitivity could be characteristic of the impulsive pull-out phenomenon.

6. Conclusion

Numerical analysis and experimental results are presented on the pull-out phenomenon in fiber-enforced composite materials at the high rate of loading accompanying impulsive breakdowns. The finite element method was used assuming an inter-laminar shear layer as the interface between a fiber and the matrix. If the fiber is pulled out impulsively, the shear stress is time dependent and decays into the value under static loading. Under step pulse loading, the inter-laminar shear stress fluctuates, finally decaying into the static value. The maximum shear stress under the impulsive loading assumes a value more than 20% larger than the static value.

(A lecture given at the 5th Symposium on FRP by the Japan Society of Material Science, May 31, 1979).

REFERENCES

1) S. Shimamura, Enforced Plastics 18, 410, 1972.
2) Broutman, L. J. and A. Rotem. AFOSR 72 2214 (AI) (illegible) (1972).
3) Outwater, J. O. and W.O. Carnes. Proceedings of the Army Symposium on Solid Mechanics, p. 17 (1968).
4) Lawrence, P. J. of Material Science, 7, 4 (1972).
5) Payton, R. G., J. of Applied Mech., 87, 643 (1965).
6) Timoshenko, B. P. and I. N. Goodier. Theory of Elasticity, Chap. 11 (1970) McGraw Hill Kogakusha, Md.